Journal of Machine Engineering, Vol. 17, No. 2, 2017

Received: *23 January 2017*/ Accepted: *16 April 2017* / Published online: *12 June 2017*

hardened steel, surface roughness,
cutting force, specific energy, corner radius

Wit GRZESIK[1*]
Krzysztof ZAK[1]
Roman CHUDY[1]

INFLUENCE OF TOOL NOSE RADIUS ON THE CUTTING PERFORMANCE AND SURFACE FINISH DURING HARD TURNING WITH CBN CUTTING TOOLS

In this paper the basic cutting characteristics such as cutting forces, cutting power and its distribution, specific cutting energies and friction were determined as functions of variable tool corner radius ranging from 400 to 1200 μm and the cutting speed ranging from 150 m/min to 270 m/min for a hardened 41Cr4 alloy steel of 55±1 HRC hardness in finish turning steel using chamfered CBN tools. Moreover, selected roughness profiles produced for different tool corner radius were compared and appropriate surface roughness parameters were determined. The measured values of Ra and Rz roughness parameters were compared with theoretical values and springback effect was taken into account.

1. INTRODUCTION

Hard machining has been established an innovated machining technology for various highly-loaded machine components made of hardened steels, such as geared shafts, bearing and hydraulic components, which need a high quality surface finish and special functional properties [1-4]. Predominantly, scientific and engineering issues of hard turning cover such problems as cutting mechanics, chip formation, tool wear, surface integrity and part accuracy [1-2]. Unfortunately, surface finish in hard machining resulting from e specific action of the cutting edge with a high negative rake angle is still a great challenge and it is an important objective of hard machining research and practice. Moreover, it is a process with large energy consumption and low energy efficiency [1,5] because the energy consumption increases distinctly due to extreme high hardness of the material machined and high negative rake angle of the CBN cutting tool used. In addition, the machined surface is evidently generated under severe influence of friction and excessive ploughing action of the cutting edge with the spring back effect. In addition, hard machining is distinguished by dominating passive force in comparison to conventional turning for which the radial force F_p=(0.3-0.5)F_c. Consequently, the radial force should be considered

[1] Opole University of Technology, Faculty of Mechanical Engineering, Opole, Poland
[*] E-mail: w.grzesik@po.opole.pl

in static and dynamic behaviour of the machining system and total energy consumption. This specific issue becomes more important when machining with CBN cutting inserts of large nose radius of 800 and 1200 μm [6].

As a result, for cutting tools with a corner radius equal to or higher than 1.2 mm uncut chip thickness decreases which intensifies ploughing interaction between the cutting edge and the subsurface layer and, as a result, material side flow [7-8].In this study, cutting forces, cutting power consumption, friction and surface finish were investigated under the variable tool nose radius and cutting speed in turning of 41Cr5 (AISI 5140) hardened steel.

2. EXPERIMENTAL DETAILS

2.1. CONDITIONS OF MACHINING TESTS

In this investigation hard turning trials were performed using hardened 41Cr4 alloy steel with 55±1 HRC hardness and CBN cutting tool inserts of CB 7015 grade and TNGA configuration by Sandvik Coromant. The average cutting edge radius was equal to r_n=10 μm and the chamfer rake angle was γ_{cf}=-30°. Three cutting tool inserts with variable tool corner radius of r_ε= 400, 800 and 1200 μm were selected. Cutting parameters include three variable cutting speeds of v_c=150, 210 and 270 m/min, constant feed rate of f=0.1 mm/rev and constant depth of cut of a_p=0.2 mm. Machine tool was a CNC turning center, Okuma Genos model L200E-M.

2.2. MEASUREMENTS AND COMPUTATIONS OF CUTTING FORCES AND SURFACE ROUGHNESS

Surface roughness produced on hardened steel specimens was measured by means of the stylus method using a TOPO-01P contact profilometer with a diamond stylus tip of 2±0.5 μm radius. A set of 2D roughness parameters was determined and surface profiles were visualized using a Digital Surf, Mountains®Map package. Three components of the resultant cutting force F_c, F_f and F_p were measured using a three-component Kistler dynamometer (model 9129A) and consumed energy recording system installed on the lathe. The measured signals were processed with a sampling rate of f=1 kHz and a low-pass filter with a cut-off frequency of f_c=300 Hz [7-8]. They were transformed into the l_{mn} coordinate system using three transformation matrixes described in Ref. [9] in order to determine the friction coefficients for the rake face. It is determined as follows

2.3. COMPUTATIONS OF FRICTION, SPECIFIC CUTTING ENERGIES AND FRICTION COEFFICIENT

The friction coefficients for the rake face is determined as follows:

$$\mu_\gamma = \frac{F_n}{F_m} = \frac{F_\gamma}{F_{\gamma N}} \tag{1}$$

where F_γ is the friction force (equal the F_n force parallel to the rake face and normal to the cutting edge) and $F_{\gamma N}$ is the normal force on the rake face (equal to the F_m force normal to the cutting edge and the rake face).

The *lmn* coordinate system is obtained by three subsequent rotations of the *xyz* coordinate system: the first by the angle κ_r around the *z* axis, the second by the angle λ_s around the *x* axis and the third by the angle γ_n around the *y* axis [8].

Specific cutting e_c and ploughing e_p energies are calculated based on the equivalent cutting edge of the length l_k and the mean uncut thickness (UCT) h_m ($A_c=h_m \times l_k$) [7-8]. Hence

$$e_c = F_c / A_c \tag{2a}$$

$$e_p = F_p / A_c \tag{2b}$$

The total specific cutting energy (e_t) is the sum of its components e_c and e_p expressed by relevant Eqns. 2a and 2b, i.e. $e_t=e_c+e_p$.

The elastic recovery of the machined surface is determined using the following equation [10].

$$\delta_s = r_n \left(1 - \frac{1+\mu_\gamma}{\sqrt{2\left(1+\mu_\gamma^2\right)}} \right) \tag{3}$$

2.4. COMPUTATIONS OF THEORETICAL ROUGHNESS HEIGHT

The theoretical values of roughness height were determined using both the classical circle model (Eq. 4) and the Brammertz formula (Eq. 5) which additionally considers the minimum UCT (it was assumed that $h_{min}=0.1r_n=1$ μm) and, in consequence, a small unremoved area of the rough machined surface.

$$Rzt = \frac{f^2}{8r_\varepsilon} \tag{4}$$

$$Rzt^B = \frac{f^2}{8r_\varepsilon} + \frac{h_{min}}{2}\left(1 + \frac{r_\varepsilon h_{min}}{2}\right) \tag{5}$$

3. EXPERIMENTAL RESULTS AND DISCUSSION

3.1. CUTTING FORCES AND CUTTING POWER

As shown above three components F_c, F_f and F_p of the resultant cutting force were recorded during hard turning tests for all sets of variable machining conditions using a piezoelectric dynamometer. Simultaneously, the cutting power P_c and cutting energy E_c were recorded using a special measurement system 5]. The changes of force components resulting from variations of the tool corner radius and cutting speed are presented in Fig. 1. As shown in Fig. 1a and 1c the minimum values of the cutting and passive forces were

revealed for the tool corner radius of 400 and 1200 μm respectively. On the other hand, the minimum values of the feed force were recorded for the tool corner radius of 800 μm (Fig. 1b). It should be noted that the values of passive force exceed distinctly the corresponding values of cutting force F_c (Fig. 1a vs. Fig. 1c). The ratio of F_p/F_c varies from 1.10 for lower tool corner radius of 400 μm to 1.45-1.55 for higher values of r_ε. Its highest value was determined for r_ε=800 μm and the cutting speed of 210 m/min. A small decrease of the passive force observed in Fig. 1c for the maximum tool corner radius of r_ε=1200 μm and higher cutting speeds of 210 and 270 m/min probably results from the thermal softening of subsurface layer occurring at higher interface temperature and the onset of material side flow documented on the recorded surface profiles (see Fig. 5). This specific force resolution in hard machining causes the relevant changes in both cutting power/energy consumption and friction due to an intensive ploughing effect (abnormal value of the passive force F_p) and the generation of surface roughness.

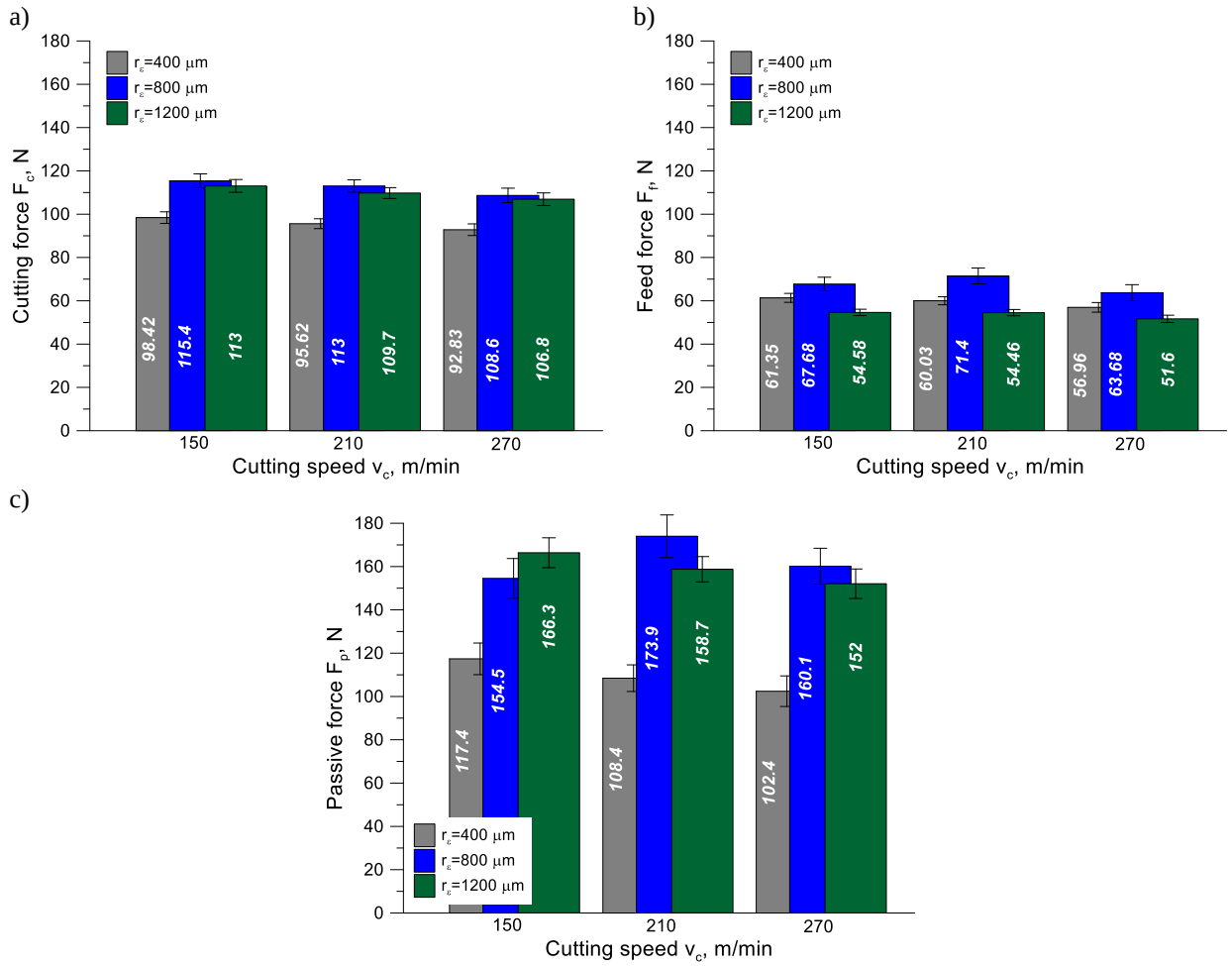

Fig. 1. Changes of F_c (a), F_f (b) i F_p (c) componential forces for variable tool nose radius and cutting speed

The changes of the cutting power $P_c=F_c \times v_c$ recorded for different tool corner radiuses are shown in Fig. 2a. The trends are similar to those observed for the cutting force *Fc* (Fig. 1a) when keeping constant cutting speed. In general, the calculated and measured values of the cutting power are practically the same. As shown in Fig. 2a the highest power

consumption was recorded for the highest cutting speed of 270 m/min but its difference resulting from employing CBN tools with the tool corner radius of r_ε=800 and 1200 μm is only about 2-5%. This effect can be pronounced when considering the influence of the tool nose radius on the roughness height *Rzt* (see Eqn. 4). The pie diagram presented in Fig. 2b indicates that in hard machining the power consumption strictly for cutting performance is about 12-14% of the total power recorded independently of the tool corner and cutting speed selected in this comparative studies

3.2. CUTTING ENERGY BALANCE

In this study energy balance of the hard cutting process is based on the total specific energy e_t and its two components including the specific cutting energy e_c and the specific ploughing energy e_p which were computed using Eqns. 2a and 2b respectively [8].

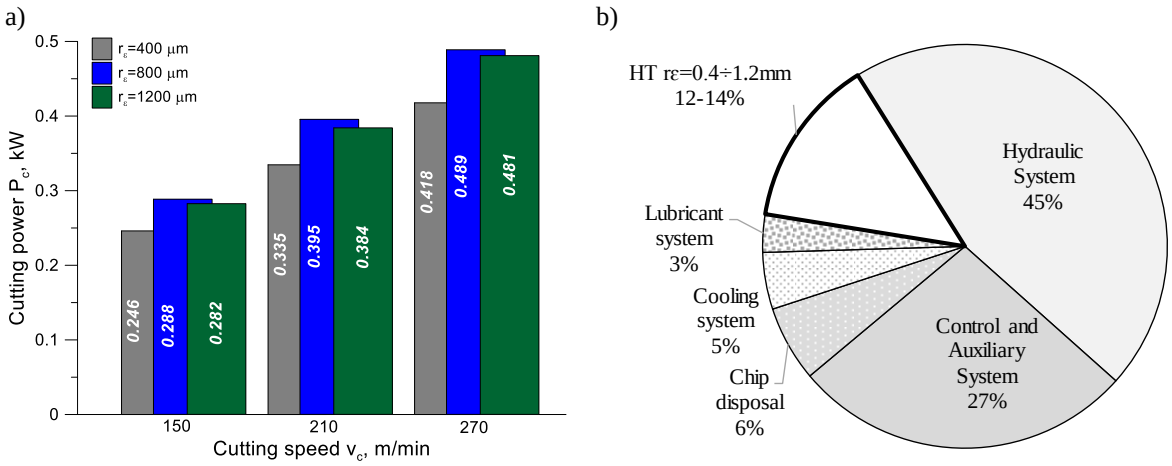

Fig. 2. Changes of cutting power for variable tool nose radius and cutting speed and its distribution (v_c=210 m/min, f=0.1 mm/rev, a_p=0.2 mm)

The changes of the total specific energy e_t, the specific cutting energy e_c and the specific ploughing energy e_p are visualized in Fig. 3a-c. Figs. 3a and 3b depict that values of e_c and e_p components depends on the tool corner radius and varied in a similar way to the changes of relevant forces. In particular, the values of e_p determined for the maximum tool corner radius of r_ε=1200 μm and higher cutting speeds of 210 and 270 m/min decrease slightly in comparison the relevant values recorded for the lower tool corner radius of r_ε=800 μm. The minimum values of about e_c =4.6-4.9 GJ/m^3 and e_p=5.1-5.9 were recorded for the minimum tool corner radius of 400 μm. These values increased up to about 5.8 GJ/m^3 for e_c (on average by 20%) and up to about 8.7 GJ/m^3 for e_c (on average by 35%). As a result, the total specific energy is about 10 GJ/m^3 for the tool corner radius of 400 μm and about 15 GJ/m^3 for the tool corner radius of 800 and 1200 μm. The cutting energy for lower tool corner radius is in the range characteristic for grinding with UCT

of about 15 μm and for higher tool corner radius is in the range characteristic for conventional turning of carbon and alloy steels with the UCT higher than 20 μm [2,8].

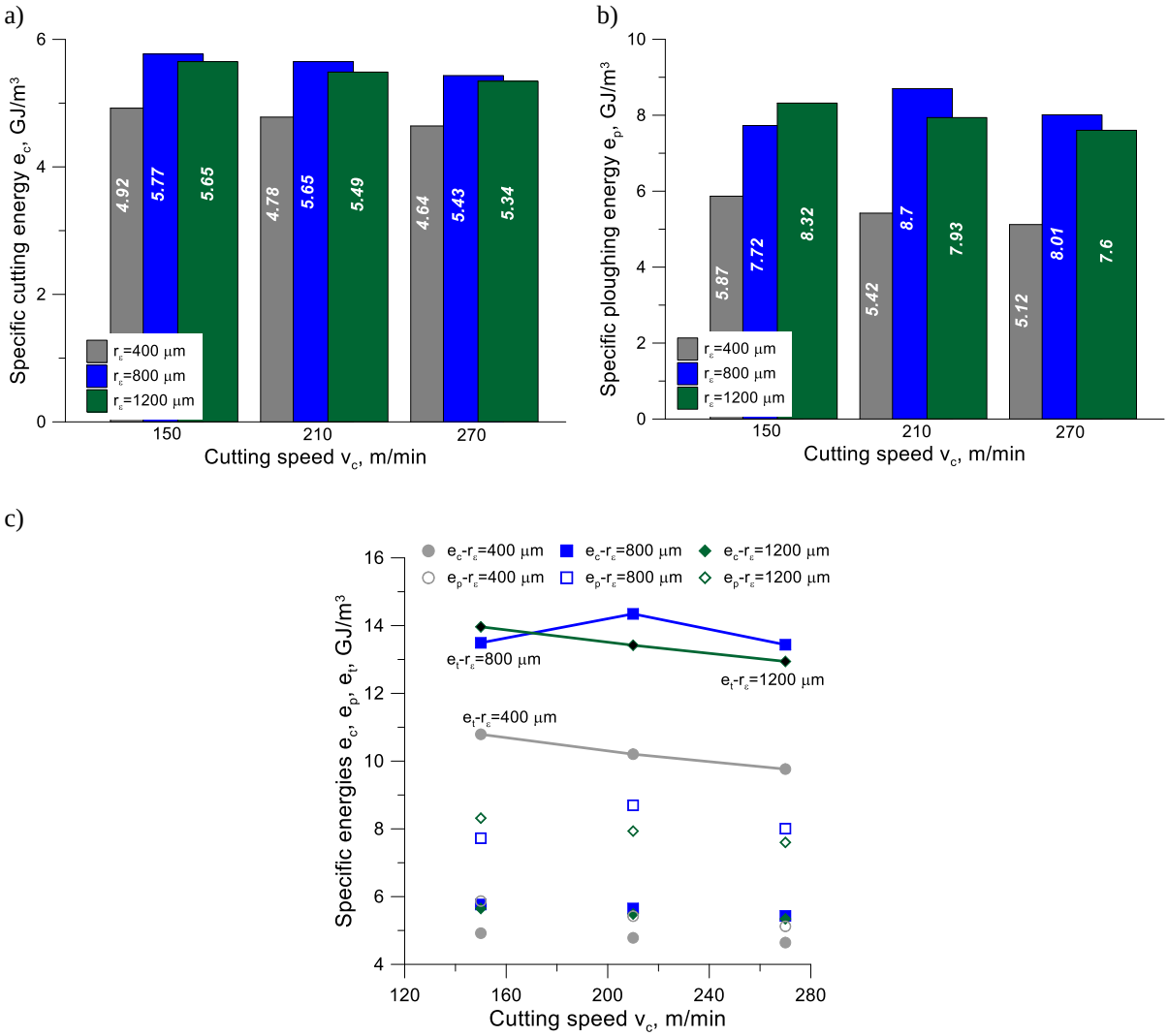

Fig. 3. Changes of e_c (a), e_p (b) and e_t (c) specific energies for variable tool nose radius and cutting speed

3.3. FRICTION AND SPRINGBACK EFFECT

Friction was characterized by the rake friction coefficient determined using Eqn. 1. Its lower values of 0.75-0.8 were obtained for the tool corner radius of 400 μm and distinctly higher values of 1.2-1.4 for the higher tool corner radius of 800 and 1200 μm, as shown in Fig. 4a. Such intensive friction and associate ploughing action of the cutting edge cause the springback (termed also elastic recovery) effect appears as documented in Ref. [10-11]. As shown in Fig. 4b its maximum values do not exceed 0.1 μm. In some cases, as for example for the tool corner radius of 400 μm and the cutting speed of 150 m/min this effect can be neglected because a very low value of δs=0.02 μm was determined.

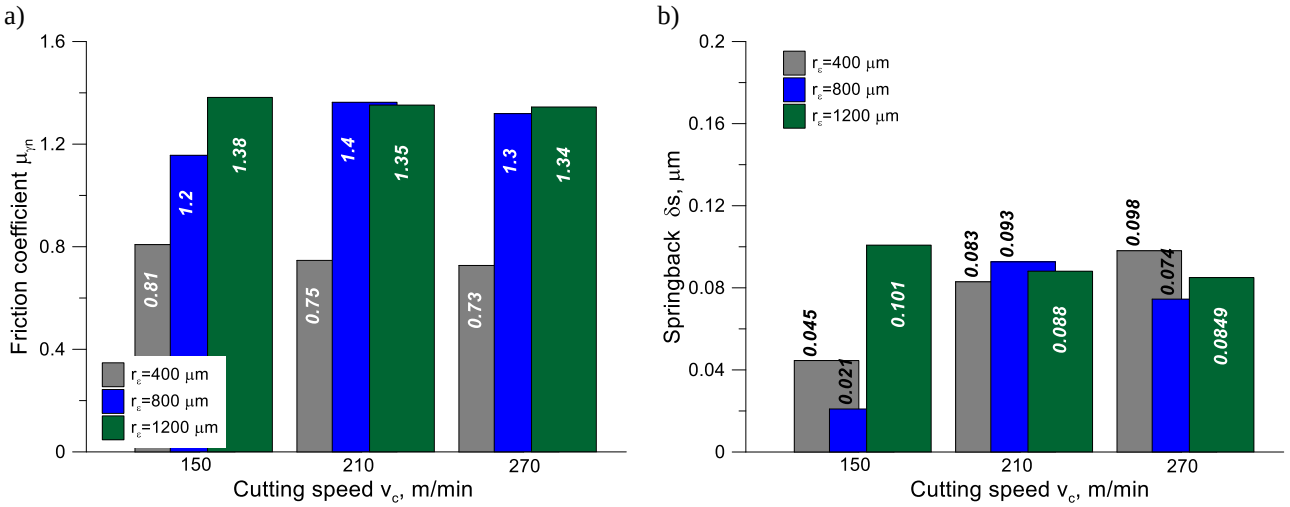

Fig. 4. Changes of friction coefficient (a) and springback effect (b) for variable tool nose radius and cutting speed

3.4. SURFACE ROUGHNESS

Representative surface profiles generated by CBN tools with different tool nose radius are shown in Fig. 5. In particular, the effect of reducing the height of irregularities due to employing higher tool corner is clear observed in Fig. 5. As shown in Fig. 6b the maximum roughness height *Rz* decreases from 3.6 μm for r_ε=400 μm, through 1.8 for r_ε=800 μm to 1.5 μm for the highest r_ε=1200 μm. As shown in Fig. 6a the relevant values of the average roughness *Ra* are equal to 0.9, 0.4 and 0.3 μm. Another specific effect resulting from employing CBN tools with a large tool corner is a visible reduction of the RMS slope *RΔq* from 4.37° for r_ε=400 μm up to 1.67° for r_ε=1200 μm (Fig. 4). Surface profiles presented in Fig. 5 are regular with distinct feed marks but especially these regularities are pronounced for the surface profile produced using CBN tool with the minimum r_ε=400 μm. When the tool corner radius increases this regularity of feed marks is distorted by small side flows observed on the left sides of all individual peaks. It can be suggested [12] that plastic flow is intensified when the cutting edge removes a very thin layer of thermally softened material. It should be noticed that the average thickness of uncut layer is equal to 47.75, 34.6 and 28.5 μm for the tool corner of r_ε=400, 800 and 1200 μm respectively.

Fig. 6b shows the agreement between measured values of *Rz* roughness parameter and its predicted values using the Brammertz formula expressed by Eqn. 5. In all cases this agreement is satisfactory and the best fitting was achieved for the maximum tool corner of r_ε=1200 μm. Some smaller differences documented for smaller tool corner radiuses can be explained in terms of the springback (elastic recovery of the machined surface) as shown in Fig. 6c. It should be noticed in Fig. 6c that the changes of springback for different machining conditions follow well the relevant changes of the *Rz* roughness parameters.

The highest elastic recovery of about 0.8-0.1 μm computed by means of Eqn. 3 was determined for the cutting speed of 210 m/min. As a result, the predicted values of *Rz* parameter can be additionally corrected by appropriate δ_s value.

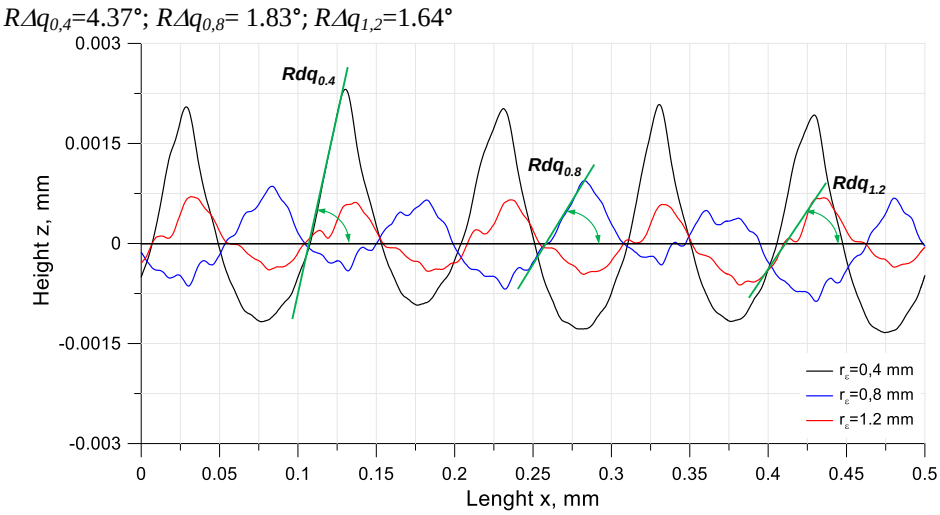

Fig. 5. Comparison of surface profiles generated by CBN tools with deferent tool corner radiuses for v_c=210 m/min

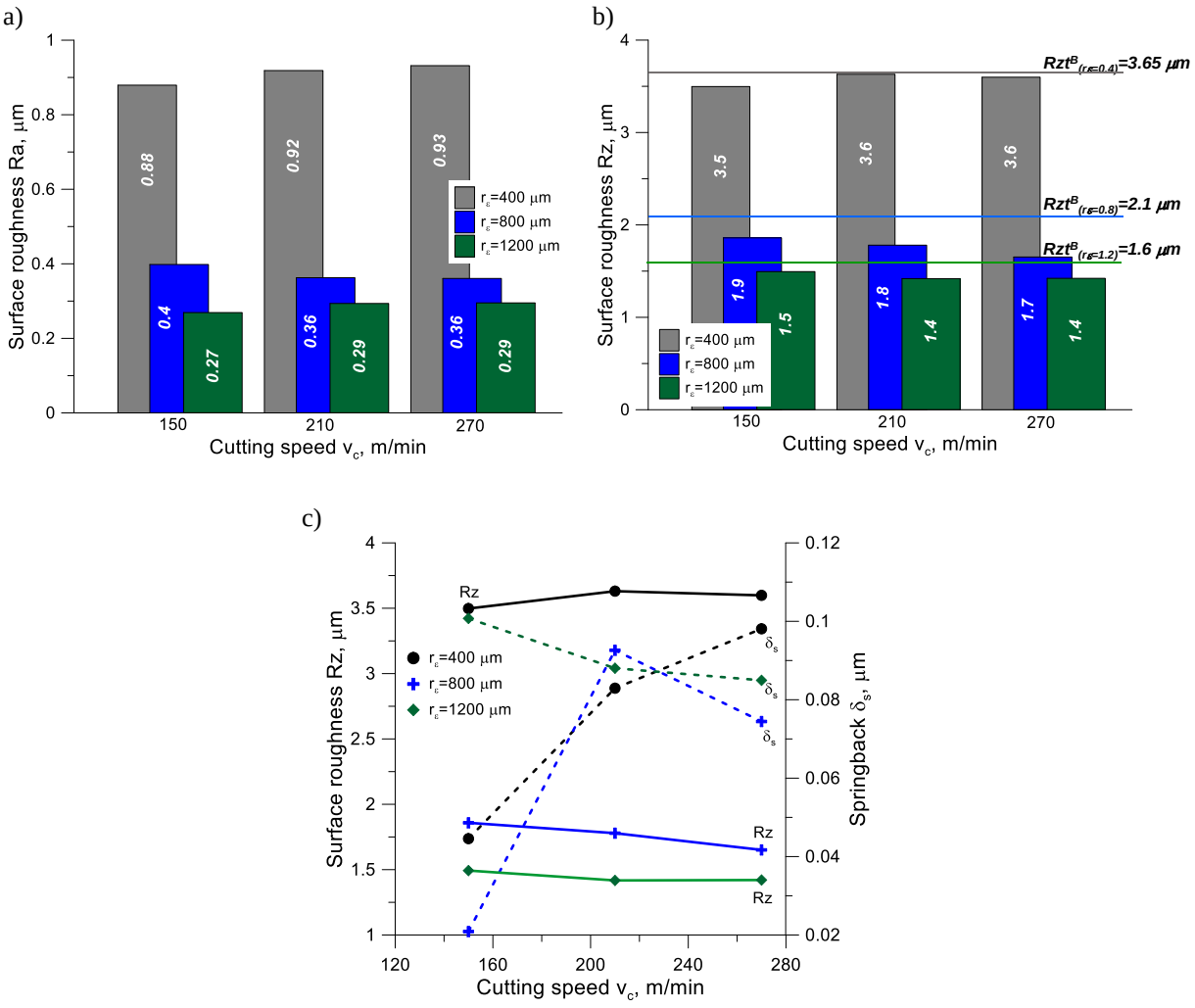

Fig. 6. Changes of *Ra* (a) and *Rz* (b) roughness parameters and dependence of *Rz* roughness parameters on springback effect (c) for variable tool corner radius and cutting speed

4. CONCLUSIONS

1. Tool corner radius ranging from 400 to 1200 μm is a decisive factor which influences both mechanical and tribological characteristics of the hard cutting process and control roughness of machined surfaces.
2. In hard turning the passive force (F_p) overestimates both cutting (F_c) and feed (F_f) forces. Under the cutting conditions used the ratio of F_p/F_c is equal to 1.10 for tool corner radius of 400 μm and increases to 1.45-1.55 for higher values of r_ε.
3. The influence of tool corner radius is that the minimum values of about e_c =4.6-4.9 GJ/m^3 and e_p =5.1-5.9 were recorded for r_ε=400 μm and they increase up to about 5.8 GJ/m^3 for e_c (on average by 20%) and up to about 8.7 GJ/m^3 for e_c (on average by 35%) for r_ε=800 and 1200 μm. From the energetic point of view hard machining coincides with grinding for higher r_ε or precision cutting operations for lower r_ε.
4. Hard machining is associated with severe friction which is produced by intensive ploughing action of the honed cutting edge. Typical values of friction coefficient are 0.75-0.8 for r_ε=400 μm and 1.2-1.4 for r_ε=800 and 1200 μm. In addition, elastic recovery of the surface take places.
5. Distinctly lower values of *Ra* and *Rz* roughness parameters were measured on hard surfaces machined using CBN chamfered cutting tools with higher tool corner radius of 800 μm and 1200 μm. The surface profiles are generated with regular feed marks and visible flashes due to plastic side flow effect.

REFERENCES

[1] DAVIM J.P., 2011, *Machining of Hard Materials*. London, Springer.
[2] GRZESIK W., 2017, *Advanced Machining Processes of Metallic Materials*, Amsterdam, Elsevier.
[3] GRZESIK W., 2016, *Influence of surface texture on the functional properties of machined components*, Journal of Machine Engineering, 15/1 15-23.
[4] GRZESIK W., 2016, *Prediction of the functional performance of machined components based on surface topography: state of the ar*t, Journal of Materials Engineering and Performance, 25/10, 4460-4468.
[5] CHUDY R., GRZESIK W., 2015, *Comparison of power and energy consumption for hard turning and burnishing operations of 41Cr4 steel*, Machine Engineering, 14/4, 113-120.
[6] CHOU Y.K, SONG H., 2004, *Tool nose effects on finish hard turning*, Journal of Materials Processing Technology, 148, 259-268.
[7] MAYER R., KÖHLER J., DENKENA B., 2012, *Influence of the tool corner radius on the tool wear and process forces during hard turning*, International Journal of Advanced Manufacturing Technology, 58, 933-940.
[8] GRZESIK W., DENKENA B., ZAK K., GROVE T., BERGMANN B., 2016, *Energy consumption characterization in precision hard machining*, International Journal of Advanced Manufacturing Technology, 85, 2839-2845.
[9] GRZESIK W., ŻAK K., 2014, *Assessment of friction incorporating tool wear effect*, Machine Engineering, 14/2, 5-15.
[10] GRZESIK W., 2010, *Generation and Modelling of Surface Roughness in Machining using Geometrically Defined Cutting Tools*, In: Metal Cutting. Research Advances, Nova Science Publishers, 6, 163-185.
[11] SCHAAL N., KUSTER F., WEGENER K., 2015, *Springback in metal cutting with high cutting speeds*, Procedia CIRP, 31, 24-28.
[12] KISHAWY H.A., HAGLUND A., BALAZINSKI M., 2006, *Modelling of material side flow in hard turning*, CIRP Annals - Manufacturing Technology, 55/1, 85-88.